Evidence of chaos in slab avalanches

Walter Rosenthal*
Donald Bren School of Environmental Science and Management
University of California, Santa Barbara

Kelly Elder
Rocky Mountain Research Station
USDA Forest Service
Fort Collins, Colorado

Abstract: We present evidence that slab avalanching is a chaotic process. A 20-year set of 8062 avalanches running on more than 140 paths at Mammoth Mountain was examined. The distribution of crown sizes greater than a given size is scale invariant (fractal) over the entire mountain and on individual paths. Chaotic systems often exhibit fractal statistics. We reconstruct the phase space portrait and resulting attractor for crown size on one avalanche path for the period 1982/1983 through 2001/2002. Independent measures of the attractor, including comparison against surrogate sets of stochastic data, indicate the time series is deterministic and that the attractor is chaotic.

Keywords: avalanche, chaos, fractals, attractors

1. Introduction

Are slab avalanches chaotic? Chaos results from deterministic mechanisms operating in nonlinear dynamical systems. Large differences in system evolution flow from small differences in initial conditions. Chaotic systems are therefore predictable in the short run but completely unpredictable in the long run. Short-term physical models give way to long-term probability estimates.

The 8062 avalanches recorded at Mammoth Mountain, CA since 1982/83 follow a power law of the form

$$N = Cr^{-D} \qquad (1)$$

where N is the number of crown sizes larger than linear measure r, C is a constant and D is the fractal dimension (Mandelbrot 1982). The distribution is scale-invariant with D=2.6 (Figure 1).

Fractal distributions are often exhibited by chaotic systems (*e.g.*, Turcotte 1997). They can reflect underlying chaotic processes because those processes operate over a wide range of scales without themselves having an inherent scale. Snow avalanches seem likely candidates for exhibiting chaos. Physical properties like temperature, degree of sintering within and between layers, density, vapor pressure gradients, grain size, grain shape and surface energy balance evolve at different rates from point to point over all scales during the season. There is not inherent scale to stratigraphy, or the distribution of strong and weak layers.

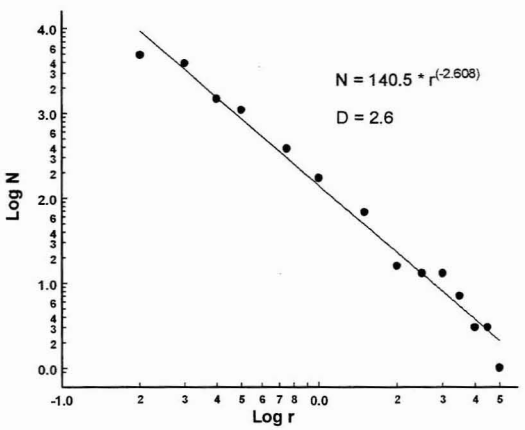

Figure 1. *Log of N, the number of crown sizes greater than r (meters) plotted against r for Mammoth Mountain, 1983-2002.*

One of the best-known signatures of chaos is the chaotic *attractor*, the map or image of the states the system assumes. The attractor exists in phase space, an n-dimensional space populated by lagged values of a single

*Corresponding author: Walter Rosenthal, P.O. Box 7457, Mammoth Lakes, CA 93546; tel: 760-935-4464; email: walter@icess.ucsb.edu

variable. For example, a lag of 1 produces a set of points in n-dimensional space with coordinates $x(t)$, $x(t+1)$, ... $x(t+(n-1))$.

The number of phase space dimensions is the *embedding dimension*. An attractor can be embedded in different numbers of dimensions; one requiring many dimensions for full expression can still be well defined and exhibit chaotic behavior in fewer dimensions.

A set of sequential points on the attractor is a *trajectory*. Chaotic trajectories have common characteristics [Williams 1997]. They are restricted to a limited region of the phase space, visit some regions more frequently than others, and it do not intersect. Trajectories that are arbitrarily close on the attractor diverge, dooming long-range prediction. Divergence is not random, however, so short-term physical modeling can be potentially fruitful, allowing deterministic or predictive applications.

In contrast, trajectories of non-chaotic attractors converge to a single set of points that are periodically revisited. The set may be a single point or many points in a complex orbit, but eventually the trajectory intersects itself and the cycle repeats.

We explored possible chaos in slab avalanching by using a single avalanche path at Mammoth Mountain in a case study. We selected crown size as the dependent variable and analyzed it for signs of chaos.

2. Methods

We examined an irregular time series of crown sizes on 416 control days during the winters of 1982/1983 through 2001/2002 on the Upper Cliffs avalanche path. Like the mountain as a whole, the number of avalanches larger than a given size r varies as a power of r, with D=2.17 (Figure 2). Smaller D indicates greater relative abundance of large avalanches than for the entire mountain.

The slope is tested with explosives every control day. It is permanently closed to skiing so the snow is not otherwise modified. Gaps between control days in a single season vary with storm cycles from a day to many weeks. If an avalanche does not occur crown size is simply recorded as "0" on the occurrence chart, but non-avalanche days are not equivalent. They are unique in loading, deposition, avalanche history and evolution. We replace "0" with negative new snow depth because crown depth is positive. Loading zones receive more new snow than the study plot, and the difference could be estimated from crown sizes for a given path. However, this would only introduce a constant scaling factor for the negative values, would not fundamentally affect the analysis, and was therefore ignored. To avoid singularities 1 was added to all values and the natural logarithm of this yielded the final time series (Figure 3).

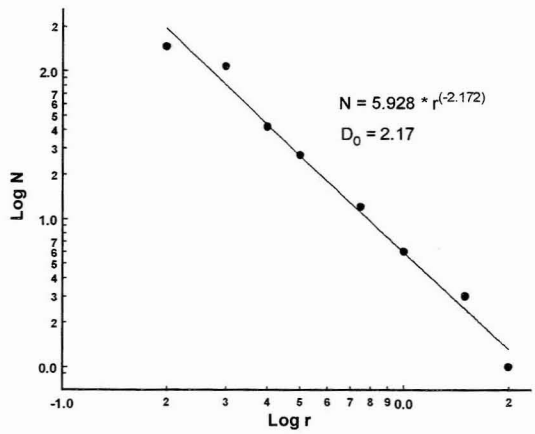

Figure 2. *Log of N, the number of crown sizes greater than r (meters) plotted against r for the Upper Cliffs avalanche path, 1983-2002.*

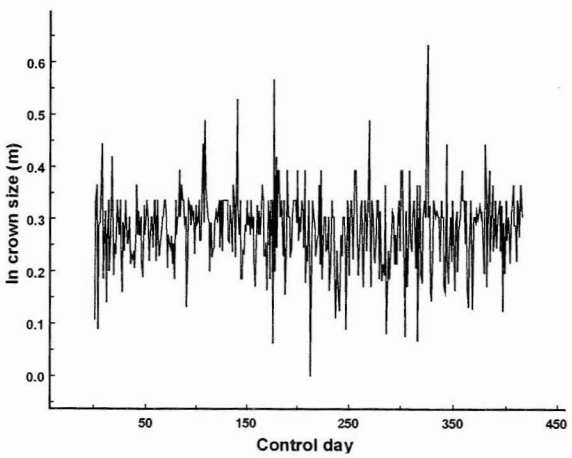

Figure 3. *Time series of crown size in the Upper Cliffs, 1982/83-2001/02*

The time series was examined for autocorrelation and periodicity. The correlogram computed to a lag of 100 shows the data to be free of autocorrelation while spectral analysis shows the data are essentially aperiodic. Both measures are within the 95% confidence interval. We therefore adopt a lag of 1 for reconstructing the attractor.

We determined embedding dimension by the method of false nearest neighbors (Kennel *et al.*, 1992). Distant

points on an attractor may appear close together when viewed in a lag space with too few dimensions. These false neighbors will separate as the attractor "unfolds" in higher dimensions until the proper embedding dimension is reached. We considered all pairs of points embedded in up to seven dimensions and tested with a wide range of tolerances. Even relaxing those tolerances and permitting the number of false nearest neighbors to reach 1% of the total number of point pairs suggests the number of embedding dimensions is at most three.

An independent estimate of embedding dimension using the correlation dimension (Grassberger and Procaccia 1983a,b) is consistent with the false nearest neighbors estimate of a three-dimensional lag space. Correlation dimension measures the probability of points being within a radius ε for each point on the attractor over a wide range of ε. It is determined by estimating the slope of the scaling region in a log plot of correlation sum C against ε, where

$$C_\varepsilon = \lim_{N\to\infty} \frac{1}{N^2} \sum_{i=1}^{N} \sum_{j=1}^{N} G\left(\varepsilon - \left|x_i - x_j\right|\right). \quad (2)$$

N is the total number of points in the set, G is the Heaviside function accepting only points of separation less than ε, and separation is computed for all pairs of points x_i and x_j on the attractor. Williams (1997) provides a clear discussion of correlation dimension.

Correlation dimension was calculated over a range of ε from 0.5% to 80% the attractor diameter, for two through ten dimensions (Figure 4). Only values up to about 10% the attractor diameter are actually useful. Correlation dimension remains approximately constant

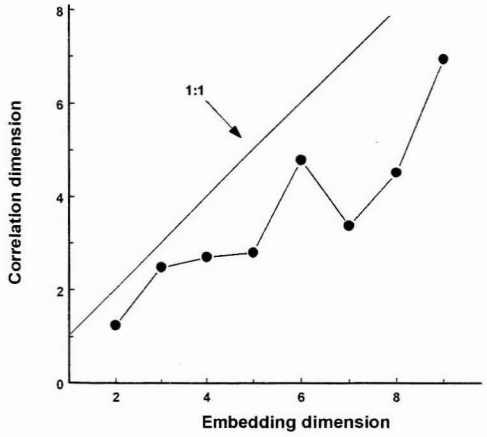

Figure 4. *Correlation dimension v. embedding dimension, Upper Cliffs crown size.*

for embedding dimensions three through five, the maximum reasonable estimate given the set size (see below), suggesting an embedding dimension of three.

The general principal behind plateau onset when plotting correlation dimension against embedding dimension is that distances between points increase geometrically with the number of dimensions. Because they are uncorrelated, random points will continue to separate and fill the available embedding space as the number of embedding dimensions is increased. They will therefore graph near the 1:1 line in a plot such as Figure 4. In contrast, deterministic data of dimension n will (ideally) remain n-dimensional as embedding dimensions are added beyond n. Onset of a distinct plateau is delayed in small datasets (Ding *et al.*, 1993) so the absence of a true flat region in the plot is expected, as is the sharp slope increase that begins at embedding dimension 6.

Lag 1 and embedding dimension three reduce the set to 414 points. Another problem arises because 17 triplets are not unique and will be intersections on the attractor even though the trajectories do not repeat. This problem is an artifact of human estimation from a distance, often under severe conditions. Recorded crown dimensions are rectangular (width and depth), though few if any crowns fit this description. Thus many recorded crown depths are identical when in fact few, if any, are. One way to compensate for this would be to randomly perturb the measurements a small amount. At this stage of investigation it is both simpler and sufficient to recognize apparent trajectory intersections as false nearest neighbors.

We applied three tests for determinism to the time series. The first used surrogate data. We generated ten sets of random numbers, each with the same length, distribution (normal), mean and standard deviation of the avalanche time series. The random series were lagged and embedded in three dimensions. Our test statistic was the correlation dimension; the null hypothesis was that there is no difference between the correlation dimensions of the crown size attractor and the attractors constructed from the lagged random series.

The second test modified that of Kaplan and Glass (1992). The principal plane in Figures 5 and 6 (discussed below) was divided into a 12-row by 17-column coarse grid of squares. For a large data set (e.g., iterations of the Lorenz equations) each pass of the trajectory through a square generates a unit vector with direction determined by where it enters and leaves a square. All unit vectors in a square are added and length of the resultant vector calculated and divided by the number of passes through a square. For deterministic data, vectors in the same region of phase space will have similar orientations and the

resultant vector will be close to unit length. Orientations for random data will tend to cancel so length of the resultant vector will approach 0 as the number of trajectory passes through a square increases. Our set is small and points are distributed sparsely about the plane. Of 204 squares, 80 contain from 1-32 points; ten squares contain two consecutive points on a trajectory and two of those contain three consecutive points. We therefore take the trajectory from each point in a square, treat each as a unit vector and calculate the resultant vector.

A third indicator of determinism is the apparent onset of a plateau at embedding dimension three in the correlation dimension measure (Figure 4). We discuss this concept further below.

3. Results

Figure 5 shows the attractor projected onto the first two principal axes. Points are not normally plotted on attractors but in this case they add definition. The attractor is a torus, exhibiting a double-lobed or bow tie distortion. Figure 6 plots the vector from each point on the attractor toward the following point; arrow length is normalized to largest distance between consecutive points.

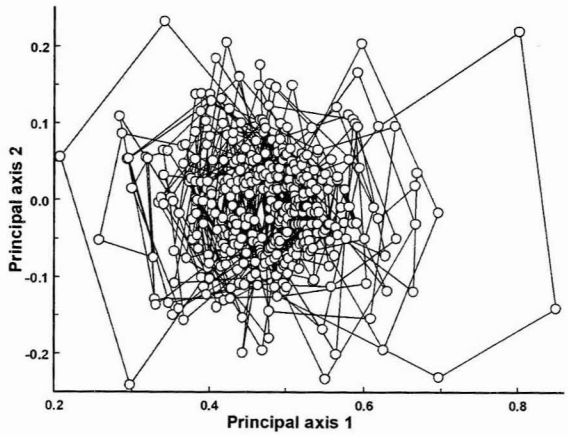

Figure 5. *The attractor and data for avalanche crown size projected on the first two principal components axes.*

Circulation is clockwise around a central void, as it sometime is around each of the lobes. The right lobe comprises productive avalanche cycles with size increasing to the right. The left lobe contains only negative crown sizes: storm cycles or series of storm days that failed to produce avalanches.

The attractor is projected onto the second and third principal axes in Figure 7 and is viewed from the right-hand edge of Figures 5 and 6. Circulation here is counter-clockwise. The horizontal axis (second principal component) is exaggerated 2:1 and this projection lacks

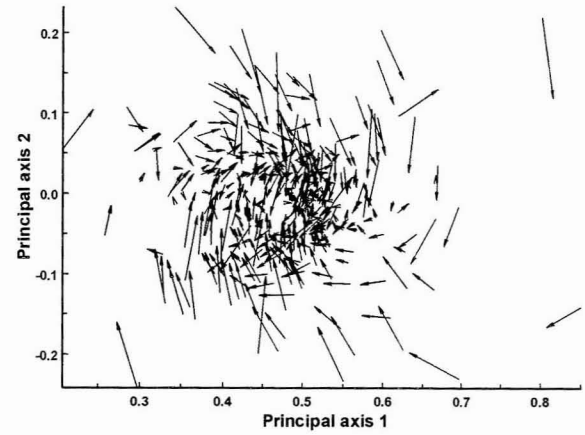

Figure 6. *The vector field showing circulation around the attractor. Arrow length is proportional to the distance between points. Data points are located at the vector tails.*

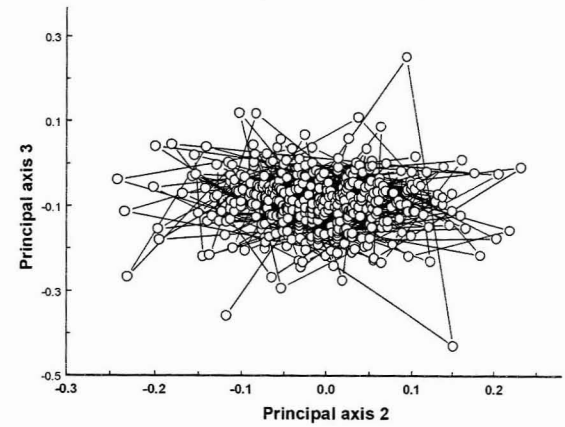

Figure 7. *The attractor and data projected onto the second and third principal axes. Note the different scales.*

the structure prominent in the first. Recall that the false nearest neighbors estimate of embedding dimension suggested at most three dimensions. The first two principal components account for only 70% of the data variance but much of the noise appears to be concentrated in the third.

All three tests of determinism indicate the time series is deterministic. The first uses the ten surrogate data sets. The null hypothesis is that there is no difference in correlation dimension between the crown size attractor and the random number series. The crown size attractor correlation dimension is 2.48. The surrogate set correlation dimensions range from 3.17 to 8.14, with mean 5.39 and standard deviation 1.77. The attractor correlation dimension falls entirely outside the range of those for the surrogate sets and the null hypothesis is rejected. The higher correlation dimensions for the surrogate data indicate that the random data fill more of the available embedding space volume and points are generally more remote from one another than those on the crown size attractor.

The lengths of the resultant vectors for the second test on the gridded data produced vectors generally near unit length and are plotted in Figure 8 as a function of the number of observations in a box. This result indicates the trajectories are well aligned. Figure 9 plots the resultant vector for each box on the coarse grid. The plot also clarifies circulation in the core region of the attractor.

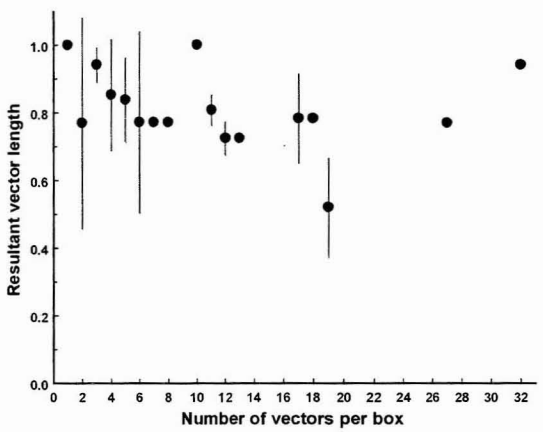

Figure 8. *Length of resultant vectors for the 12 by 17 coarse-gridding of the principal plane in Figures 5 and 6, with standard error of the estimate (whiskers).*

4. Discussion

Trajectories orbit a central void near (0.47,0.00) in Figure 5. In the right lobe point density decreases away from the center as expected from the fractal crown size distribution; small avalanches are more numerous on all scales than large ones. Decrease in point density as one moves outward into the left lobe may be explained by the fractal distribution of new snow layers measured at the study plot (not shown).

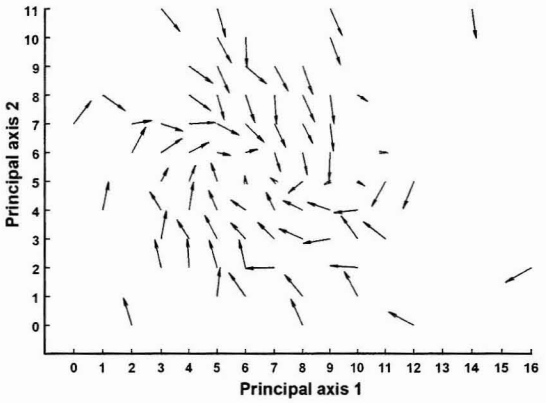

Figure 9. *The coarse-grained circulation summarized in Figure 8 plotted for each box. Resultant vectors originate at box centers, marked by ticks. Boxes are numbered 0,0 through 16,11.*

Fractal crown size distribution could result from a fractal distribution of features (bowls and gullies) comprising the avalanche paths. The primary argument against this is that the size classes are path-specific. Second, though many landscapes are fractal, Mammoth Mountain is a young volcano built by a series of eruptions ending 50,000 years ago. It is characterized by smooth pumice slopes and is not heavily eroded. Five evenly spaced elevation contours from 2900m to 3300m were chosen from a 7.5' USGS topographic map of the mountain and their lengths were measured with a divider counting measure [Mandelbrot 1982] on scales from 50 to 3000 m. Contours quickly approach a constant length; the terrain is not scale invariant and therefore not fractal.

We caution that our data set, like most from earth science, is small by chaos standards. Most measures of chaos assume samples numbering many thousands. This small sample size is a problem for statistical tests of chaos and for evaluation of the attractor. An aperiodic orbit in a small data set may prove periodic when the set is extended to tens of thousands of cases.

We must therefore view the results in Figure 4 cautiously. Estimates of correlation dimension can be spurious for small data sets where few points lie within small radii relative to the size of the attractor and it is difficult to fit a line to relevant points. The maximum embedding dimension reasonably estimated from correlation dimension is $2 \log N / \log(1/r)$, where r is the maximum radius within which pairs of points are evaluated and N is the number of points (Eckmann and Ruelle 1992). Estimated embedding dimension must be

significantly smaller than this. For 416 points and r equal to 0.1 the attractor diameter, the upper limit on embedding dimension is 5.2. Another undesirable consequence of a small data set is a short plateau beyond $\varepsilon = 3$, followed by increase in correlation dimension estimate at higher embedding dimensions (Ding 1993).

Small set size is further complicated by noise. Crown depth is not measured against a scale but estimated at a distance by blasters in the field under difficult conditions. Estimates differ between observers, but the set is large enough that these errors should average out even over short periods of time. Other sources of human error are the tendency to round estimates to the nearest few inches or foot (depending on size), under-reporting of small avalanches and recording results late in the day or not at all because of ensuing pressures of the day.

We would like additional reliable measures of the attractor. For example, a quantitative measure of trajectory divergence is λ, the Lyapunov exponent. Small set size precludes this evaluation technique. Reliable calculation of λ requires the square of the number of points required for the correlation dimension [Eckmann and Ruelle 1992], or over 100,000 points in our case.

If slab avalanching is a chaotic process, a major implication is that attempts to physically model long-term slab evolution and potential release are doomed because initial conditions below the resolution of the model will diverge unpredictably. Short-range forecasts could be based on physics alone but long-range models would have to incorporate probability, as in ensemble weather forecasts where initial conditions are varied in a suite of models to estimate likely weather patterns a week or two in the future.

5. Acknowledgement

We wish to thank Mammoth Mountain Ski Area and the Mammoth Mountain Ski Patrol for providing weather and avalanche records and for their continuing support of this research.

References

Ding, M. and C. Grebogi and E. Ott and T. Sauer and J.A. Yorke, Plateau onset for correlation dimension: When does it occur? Physical Review Letters **70**, p. 3872, 1993.

Eckmann, J.-P. and D. Ruelle, Fundamental limitations for estimating dimensions and Lyapunov exponents in dynamical systems. Physica D **56**, p. 185, 1992.

Grassberger, P. and I. Procaccia,
1983a: Characterization of strange attractors, Physical Review Letters **50**(5), p.365, 1983.

1983b: Measuring the strangeness of strange attractors, Physica D **9**, p. 189, 1983.

Kaplan, D.T. and L. Glass, Direct test for determinism in a time series, Physical Review Letters **68**, p. 427, 1992.

Kennel, M.B. and R. Brown and H.D.I. Arabanel, Determining embedding dimension for phase-space reconstruction using a geometrical construction. Phys. Rev. A **45**, p. 3403, 1992.

Mandelbrot, B.B., *The Fractal Geometry of Nature*, W. H. Freeman, New York 1982. 1983 edition.

Turcotte, D.L., *Fractals and Chaos in Geology and Geophysics*, Cambridge University Press, 1997. 2nd Edition.

Williams, G.P., *Chaos Theory Tamed*, Joseph Henry Press, Washington, D.C. 1997.